The Astrophysical Journal Supplement Series, 207:26 (7pp), 2013 August doi:10.1088/0067-0049/207/2/26

THE MAGNESIUM ISOTOPOLOGUES OF MgH IN THE $A^2\Pi$–$X^2\Sigma^+$ SYSTEM

Kenneth H. Hinkle[1], Lloyd Wallace[1], Ram S. Ram[2], Peter F. Bernath[2,3], Christopher Sneden[4], and Sara Lucatello[5]
[1] National Optical Astronomy Observatories, P.O. Box 26732, Tucson, AZ 85726, USA; hinkle@noao.edu, wallace@noao.edu
[2] Department of Chemistry, University of York, Heslington, York YO10 5DD, UK; rr662@york.ac.uk
[3] Department of Chemistry and Biochemisty, Old Dominion University, Norfolk, VA 23529, USA; pbernath@odu.edu
[4] Department of Astronomy, University of Texas at Austin, Austin, TX 78712, USA; chris@verdi.as.utexas.edu
[5] INAF, Osservatorio Astronomico di Padova, Vicolo dell'Osservatorio 5, I-35122 Padova, Italy; sara.lucatello@oapd.inaf.it
Received 2013 March 13; accepted 2013 May 12; published 2013 July 19

ABSTRACT

Using laboratory hollow cathode spectra we have identified lines of the less common magnesium isotopologues of MgH, ^{25}MgH and ^{26}MgH, in the $A^2\Pi$–$X^2\Sigma^+$ system. Based on the previous analysis of ^{24}MgH, molecular lines have been measured and molecular constants derived for ^{25}MgH and ^{26}MgH. Term values and linelists, in both wavenumber and wavelength units, are presented. The $A^2\Pi$–$X^2\Sigma^+$ system of MgH is important for measuring the magnesium isotope ratios in stars. Examples of analysis using the new linelists to derive the Mg isotope ratio in a metal poor dwarf and giant are shown.

Key words: molecular data – stars: abundances – stars: late-type – sunspots

Online-only material: color figures, machine-readable tables

1. INTRODUCTION

MgH is a well known molecular constituent of cool star atmospheres. The most prominent spectroscopic signature is the $A^2\Pi$–$X^2\Sigma^+$ bands in optical green spectra. Laboratory spectra of the dominant ^{24}MgH isotopologue have been analyzed in a series of papers by Shayesteh, Bernath and collaborators (Shayesteh & Bernath 2011; Shayesteh et al. 2007, 2004; Bernath et al. 1985). Most recently they have calculated new Einstein A values for the $A^2\Pi$–$X^2\Sigma^+$ and $B'\,^2\Sigma^+$–$X^2\Sigma^+$ systems (GharibNezhad et al. 2013). This work was preceded in the 1970s by the analysis of Balfour and co-workers on MgH optical and ultraviolet spectra (Balfour 1970, 1980, and references therein). In this paper we analyze laboratory spectra of the MgH A–X system to produce a much improved linelist for the two less abundant ^{25}MgH and ^{26}MgH isotopologues.

The principal motivation for the current work is to enhance the use of MgH as a probe of the astrophysically important Mg isotopes. However, a MgH linelist including all the isotopes has applications in various other projects requiring analysis of the detailed structure of the A–X bands. The A–X MgH transition can be used as probe of stellar photospheric temperature (Wyller 1961) and surface gravity (Bonnell & Bell 1993). MgH is a source of line and continuum opacity in cool dwarfs (Weck et al. 2003a, 2003b) with the A–X transition observed as cool as L4 (Reid et al. 2000). In cool dwarfs detection of MgD has been proposed to distinguish brown dwarfs from planetary mass objects (Pavlenko et al. 2008). It has been known for nearly a century that the spectrum of MgH exhibits the Zeeman effect. Almy & Crawford (1929) present an analysis of the splitting as a function of magnetic field strength for the A–X transition in laboratory spectra. Wöhl (1969) made the first observations of Zeeman effect in the MgH A–X spectrum in sunspots. The spectrum of MgH from the quiet Sun shows linear polarization due to scattering in the solar atmosphere (Mohan Rao & Rangarajan 1999). The Hanle effect in MgH lines, resulting from rotation of the polarization by weak solar magnetic fields, has been used to study the small scale solar structures in the photosphere (Asensio Ramos & Trujillo Bueno 2005). A detailed understanding of the isotopic spectrum should be especially useful in this kind of detailed spectrum synthesis.

Magnesium has three stable isotopes, ^{24}Mg, ^{25}Mg, and ^{26}Mg. The most common isotope is ^{24}Mg with the terrestrial isotopic abundance ratio of 78.99:10.00:11.01 (Catanzaro et al. 1966). The bands of the MgH $A^2\Pi$–$X^2\Sigma^+$ transition in the optical spectra of solar and later type stars hold the potential for isotopic analysis over a large range of temperatures and abundances (Cottrell 1978). Knowledge of the Mg isotopic ratio has historically come from study of the A–X transition. The first study of Mg isotopes in cool stars was conducted by Boesgaard (1968) using photographic coudé spectra (see Yong et al. 2003, and references there in). Increases in resolving power and signal-to-noise ratios (S/Ns) of modern telescopes/spectrographs have led to studies of Mg isotopic abundances in a variety of field and globular cluster stars (see references in Yong et al. 2006; Meléndez & Cohen 2007).

The magnesium isotopic ratios are probes of the heavy element enrichment of the universe. In massive stars ^{25}Mg and ^{26}Mg are produced during He burning by ^{22}Ne(α, n)^{25}Mg followed by neutron capture conversion of some ^{25}Mg into ^{26}Mg. ^{24}Mg is produced during carbon burning. However, explosive carbon burning can produce all three Mg isotopes. The ^{22}Ne(α, n)^{25}Mg reaction also is active in thermally pulsing stars. Tomkin & Lambert (1980) note that a common feature of these sources of Mg is the dependence of ^{25}Mg and ^{26}Mg production on the initial abundance of heavy elements. The production of ^{24}Mg is nearly independent of the initial abundance of heavy elements. Low abundances of heavy elements will result in more ^{24}Mg relative to ^{25}Mg and ^{26}Mg.

Measuring the Mg isotopic ratio from MgH lines is a difficult observational problem. Cool stellar spectra in the 5000–5200 Å region are very complex, as can be seen in line identifications by Hinkle et al. (2000) of the K giant Arcturus. The lowest-lying MgH A–X system rotational lines are spin doublets divided into three hyperfine transitions due to the nuclear spin. The isotopic splitting of these lines is small, typically 0.1 Å for the (0, 0) band. High resolution, high S/N, and spectrum synthesis are required to measure the isotopic ratio. Isotopic splitting for the

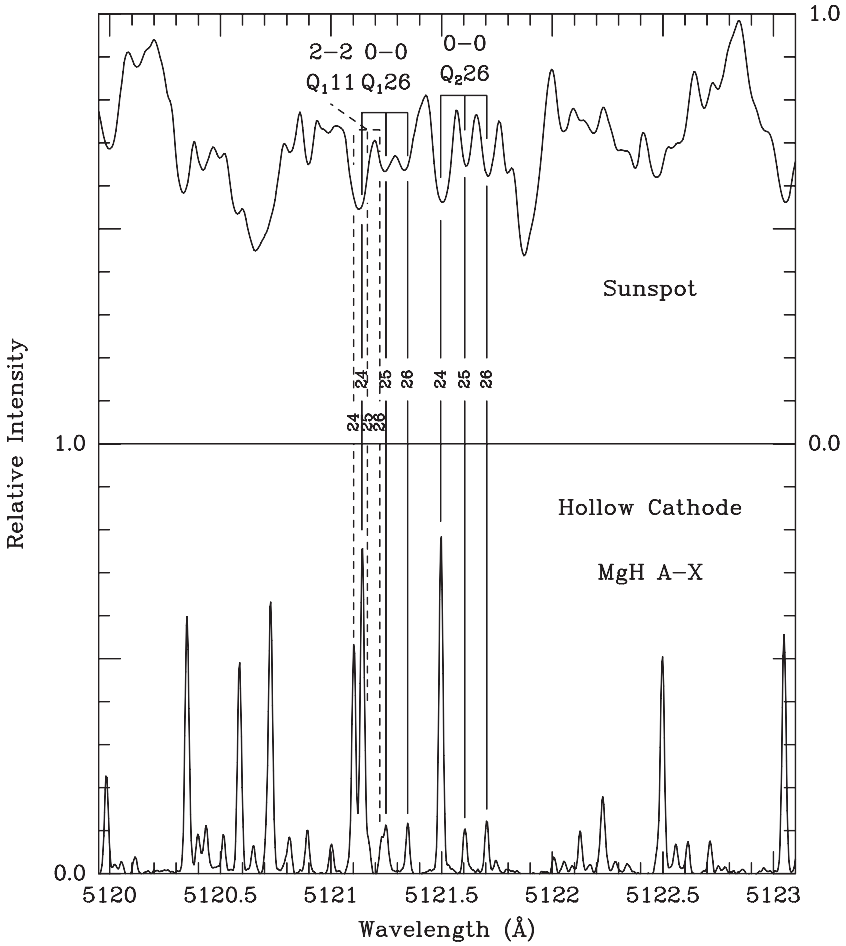

Figure 1. Unblended MgH lines from the three isotopologues in the hollow cathode spectrum compared with a sunspot spectrum. The intensity normalization of the laboratory spectrum is arbitrarily chosen to best display the MgH lines, and that of the sunspot spectrum is set to approximate the local continuum level. The abscissa is wavelength in Å units in air.

weaker (0, 1) and (1, 2) bands is larger (0.4 Å) but the spectrum is complex with many blends. Use of other transitions, e.g., $B'\,^2\Sigma^+$–$X^2\Sigma^+$ (Wallace et al. 1999), has not proved generally useful since the stronger A–X lines are required to probe the weak isotopes.

In the following section we present our analysis of the ^{25}MgH and ^{26}MgH isotopologue spectra. Spectroscopic constants and term values are presented. Tables of line wavenumbers and wavelengths are also presented. In the final section we apply the new linelist to the spectrum synthesis of a dwarf and giant star.

2. OBSERVATION AND ANALYSIS

Rotationally resolved lines within the $A^2\Pi$–$X^2\Sigma^+$ state transition of the ^{25}MgH and ^{26}MgH isotopologues were measured from spectra recorded by J. Black, P. F. Bernath, C. R. Brazier, and R. Hubbard in 1984 (National Solar Observatory (NSO) archive reference 1984/03/13/#2) with the 1 m Fourier transform spectrometer associated with the McMath-Pierce Solar Telescope of the NSO at Kitt Peak. The instrumental setup used using a water-cooled Mg hollow cathode lamp operated with 300 mA current at 200 V. A slow flow of about 0.914 torr of Ar with a trace of H_2 produced the observed spectrum of MgH. The experiment and the analysis were focused on determining wavelength information. Intensities were not analyzed. The spectral line positions were extracted from the observed spectra using a data reduction program called PC-DECOMP developed by J. Brault. The peak positions were determined by fitting a Voigt line shape function to each spectral feature. Two short intervals extracted from the hollow cathode spectrum are illustrated in Figures 1 and 2. A detailed discussion of the reduction of a ^{24}MgH spectrum recorded during the same observing session using the same software package can be found in Bernath et al. (1985).

In addition to the MgH bands a number of Ar lines are also present in the spectra. The spectral line positions were calibrated using the Ar line measurements of Whaling et al. (2002) as corrected by Sansonetti (2007). The line positions are expected to be accurate to 0.005 cm^{-1} or better except those lines overlapped by the much stronger ^{24}MgH isotopologue.

Spectra of the main isotopologue, ^{24}MgH, have been studied in detail by Bernath et al. (1985) and later by Shayesteh & Bernath (2011). Therefore, the aim of the present work was to provide improved measurements of the weaker isotopologues, ^{25}MgH and ^{26}MgH in the $\Delta v = 0$ and $\Delta v = -1$ sequence bands. In the beginning some rotational lines of the two weaker isotopologues were measured with the help of lines positions published by Balfour (1970). A least-squares fit of these lines was obtained using Brown's N^2 Hamiltonian (Brown et al. 1979). The matrix elements for the $^2\Pi$ state are provided by Amiot et al. (1981) and those of the $^2\Sigma$ state are provided by Douay et al. (1988). After the initial fit, the positions of a number of higher J rotational lines were predicted using the fitted spectroscopic parameters and the line assignments were

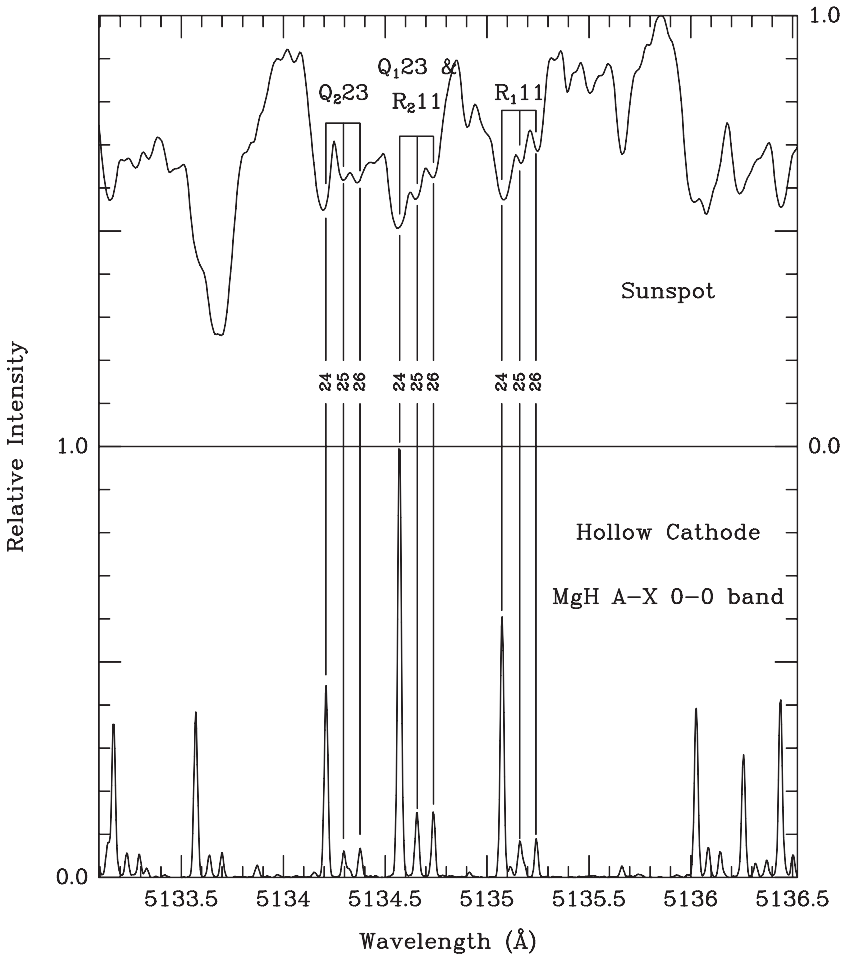

Figure 2. A second spectral region, as in Figure 1, showing relatively unblended MgH lines.

extended to higher J. These predictions were very helpful in identifying the rotational lines in the head-forming P_1 and P_2 branches which were difficult to find because of overlapping near the band heads.

Rotational lines belonging to all six main branches R_1, R_2, Q_1, Q_2, P_1, and P_2 were measured in the spectra of the 0–0, 0–1, 1–1, and 1–2 bands of both isotopologues. However, in the 2–2 and 2–3 bands only a few lines of the R_1 and R_2 branches were identified in addition to the Q_1 and Q_2 branches. The P_1 and P_2 lines could not be assigned in these two bands; the lines are very weak and the line positions severely overlap. The measurements in these bands have higher uncertainty compared to the other bands because of the poor S/N. In the 0–0 band of the two isotopologues the lines up to $J = 35.5$ (in the Q_1 branch) were identified and included in the final fit. In the 0–1, 1–1, and 1–2 bands the rotational lines were identified up to $N = 28.5$. However the observations were limited to $N < 18.5$ in the 2–2 and 2–3 bands.

The spectroscopic parameters T_v (except $v = 0$), B_v, D_v, H_v, γ_v, and γ_{Dv} were determined in the $X^2\Sigma^+$ ground state. The spectroscopic parameters T_v, A_v, γ_v, γ_{Dv}, B_v, D_v, H_v, q_v, q_{Dv}, p_v, and p_{Dv} were determined in the $A^2\Pi$ state. A number of higher order constants such as H_v, γ_{Dv}, and p_{Dv} were not varied for the $v = 2$ vibrational level of the $A^2\Pi$ state of the two isotopologues because of limited data. In the final fits infrared vibration-rotation measurements of ^{25}MgH and ^{26}MgH isotopologues by Shayesteh et al. (2004) were included. Hyperfine-corrected pure rotational frequencies for ^{25}MgH and ^{26}MgH were also included from millimeter-wave measurements by Bucchino & Ziurys (2013) and Ziurys et al. (1993) respectively.

The spectroscopic constants of the $A^2\Pi$ electronic state of ^{25}MgH and ^{26}MgH isotopologues are provided in Tables 1–4. Term values are provided in Tables 5–8. Line positions in vacuum wavenumbers (cm^{-1}) are given in Table 9 and in air wavelengths (Å) in Table 10. The air wavelengths were computed from the vacuum wavenumbers using the Edlén (1953) equation for the index of refraction of air at standard temperature and pressure. For the convenience of the reader we have included wavenumbers and wavelengths for ^{24}MgH from the work of Shayesteh & Bernath (2011). The $O - C$ values are provided for all three isotopologues for observed lines.

In Figures 1 and 2 the hollow cathode spectrum is compared to the sunspot spectra of Wallace & Livingston (2005).[6] For the MgH lines illustrated ($N = 11$ and 26) the Zeeman effects are negligible for the sunspot magnetic fields. The complexity of the cool star spectra is apparent. The 5121 Å lines are bracketed by an Ti I and Fe I line. The 5134 Å lines are bracketed by an Fe I and Cr I line. Additionally, weak C_2 lines are plentiful in these spectral regions. In spite of this atomic and molecular transition complexity, the detailed concordance between the emission wavelengths of all MgH isotopologues and sunspot absorption features argues for the reliability of our ^{25,26}MgH line measurements.

[6] Available digitally at http://diglib.nso.edu/ftp.html.

Table 1
Spectroscopic Constants[a,b] of the ^{25}MgH $X^2\Sigma^+$ State

v	0	1	2	3
T_v	0.0	1430.87095(36)	2798.56947(57)	4099.3397(15)
B_v	5.72732130(57)	5.5465244(66)	5.359247(11)	5.161918(44)
$D_v \times 10^4$	3.52662(11)	3.53874(31)	3.58017(52)	3.6619(33)
$H_v \times 10^8$	1.28480(98)	1.0994(36)	0.8116(66)	0.225(74)
$\gamma_v \times 10^2$	2.63505(28)	2.4984(59)	2.3588(87)	2.1296(82)
$\gamma_{Dv} \times 10^5$	−0.658(15)	−0.595(21)	−0.540(30)	...

Notes.
[a] Units cm^{-1}.
[b] One standard deviation error in the last two digits are in parentheses.

Table 2
Spectroscopic Constants[a,b] of the ^{26}MgH $X^2\Sigma^+$ State

v	0	1	2	3
T_v	0.0	1429.85210(38)	2796.62960(58)	4096.58463(88)
B_v	5.71888234(33)	5.5384820(68)	5.351609(11)	5.154755(21)
$D_v \times 10^4$	3.51838(29)	3.53002(39)	3.56972(56)	3.6476(10)
$H_v \times 10^8$	1.3121(49)	1.1242(56)	0.8179(77)	...
$\gamma_v \times 10^2$	2.631360(89)	2.4957(60)	2.3387(87)	2.186(19)
$\gamma_{Dv} \times 10^5$	−0.787(16)	−0.740(23)	−0.591(31)	−0.60(13)

Notes.
[a] Units cm^{-1}.
[b] One standard deviation error in the last two digits are in parentheses.

Table 3
Spectroscopic Constants[a,b,c] of the ^{25}MgH $A^2\Pi$ State

v	0	1	2
T_v	19278.53011(98)	20812.2201(12)	22277.5332(25)
A_v	35.0068(50)	35.0357(45)	35.002(10)
$\gamma_v \times 10^2$	−1.398(15)	−1.224(18)	−1.163(26)
$\gamma_{Dv} \times 10^6$	4.62(31)	8.36(49)	...
B_v	6.0850599(96)	5.895079 (18)	5.697575(46)
$D_v \times 10^4$	3.69033(26)	3.72328(68)	3.7549(14)
$H_v \times 10^8$	1.3196(18)	1.1781(68)	...
$q_v \times 10^3$	1.8553(69)	1.467(12)	0.983(62)
$q_{Dv} \times 10^6$	−1.148(12)	−1.876(31)	−6.81(23)
$p_v \times 10^2$	2.652(21)	2.282(26)	2.282*
$p_{Dv} \times 10^5$	−1.085(44)	−1.566(80)	...

Notes.
[a] Units cm^{-1}.
[b] One standard deviation error in the last two digits are in parentheses.
[c] Asterisks mark fixed values.

Table 4
Spectroscopic Constants[a,b,c] of the ^{26}MgH $A^2\Pi$ State

v	0	1	2
T_v	19278.50643(92)	20811.1036(12)	22275.4308(30)
A_v	35.0297(51)	35.0242(44)	35.006(11)
$\gamma_v \times 10^2$	−1.308(15)	−1.254(18)	−1.256*
$\gamma_{Dv} \times 10^6$	1.30(32)	8.22(56)	...
B_v	6.0760714(91)	5.886512(17)	5.689566(46)
$D_v \times 10^4$	3.68136(40)	3.71326(71)	3.7289(16)
$H_v \times 10^8$	1.3450(52)	1.2017(82)	...
$q_v \times 10^3$	1.8612(74)	1.443(13)	1.457*
$q_{Dv} \times 10^6$	−1.172(15)	−1.746(36)	−4.837(62)
$p_v \times 10^2$	2.580(22)	2.353(27)	2.458(78)
$p_{Dv} \times 10^5$	−0.810(51)	−1.919(93)	...

Notes.
[a] Units cm^{-1}.
[b] One standard deviation error in the last two digits are in parentheses.
[c] Asterisks mark fixed values.

Table 5
Term Values for the $A^2\Pi$ state of ^{25}MgH

v	N	J	F1e[a]	F1f[a]	N	J	F2e[a]	F2f[a]
0	0	0.5	19273.1942	19273.2244				
0	1	1.5	19287.3051	19287.3531	2	1.5	19318.4046	19318.4170
0	2	2.5	19312.5859	19312.6430	3	2.5	19353.9078	19353.9409
0	3	3.5	19349.5944	19349.6550	4	3.5	19401.9410	19402.0003
0	4	4.5	19398.5199	19398.5796	5	4.5	19462.2533	19462.3427

Notes. [a] Units cm^{-1}.

(This table is available in its entirety in a machine-readable form in the online journal. A portion is shown here for guidance regarding its form and content.)

3. APPLICATION OF THE NEW MgH LINE LISTS TO STELLAR SPECTRA

We have applied our new MgH line data to the spectra of two well-studied field stars. We generated synthetic spectra to compare with observed spectra of HD 25329 and Arcturus. HD 25329 is a cool metal-poor main-sequence star: $T_{\rm eff}$/log $g/v_{\rm turb}$/[Fe/H] = 4800 K/4.66/0.6/−1.84 (e.g., Bergemann & Gehren 2008). It is notable for strong CN bands and consequent nitrogen overabundance (e.g., Harmer & Pagel 1973; Sneden 1974), a rarity among unevolved metal-poor stars. Arcturus is the brightest mildly metal-poor giant (4300 K/1.50/1.5/−0.50; e.g., Bergemann et al. 2012), and as such has been spectroscopically investigated many times. Each of these stars has had previous Mg isotopic studies. The derived Mg isotopic ratios, unlike the Mg abundance, are highly insensitive to consistent variations in the adopted atmospheric parameters.

The strongest lines of the $A^2\Pi$–$X^2\Sigma^+$ system lie in the 5000–5200 Å spectral region. This wavelength domain presents

Table 6
Term Values for the $X^2\Sigma^+$ State of ^{25}MgH

v	N	J	p	Term Value[a]	N	J	p	Term Value[a]
0	0	0.5	e	0.0000	1	0.5	f	11.4269
0	1	1.5	e	11.4664	2	1.5	f	34.3118
0	2	2.5	e	34.3775	3	2.5	f	68.6246
0	3	3.5	e	68.7165	4	3.5	f	114.3399
0	4	4.5	e	114.4579	5	4.5	f	171.4241
0	5	5.5	e	171.5680	6	5.5	f	239.8351

Notes. [a] Units cm^{-1}.

(This table is available in its entirety in a machine-readable form in the online journal. A portion is shown here for guidance regarding its form and content.)

Table 7
Term Values for the $A^2\Pi$ State of ^{26}MgH

v	N	J	F1e[a]	F1f[a]	N	J	F2e[a]	F2f[a]
0	0	0.5	19273.1406	19273.1701				
0	1	1.5	19287.2414	19287.2882	2	1.5	19318.3489	19318.3611
0	2	2.5	19312.4924	19312.5479	3	2.5	19353.7925	19353.8252
0	3	3.5	19349.4513	19349.5100	4	3.5	19401.7502	19401.8087
0	4	4.5	19398.3081	19398.3656	5	4.5	19461.9703	19462.0587
0	5	5.5	19459.1192	19459.1717	6	5.5	19534.3173	19534.4391

Notes. [a] Units cm^{-1}.

(This table is available in its entirety in a machine-readable form in the online journal. A portion is shown here for guidance regarding its form and content.)

Table 8
Term Values for the $X^2\Sigma^+$ state of ^{26}MgH

v	N	J	p	Term Value[a]	N	J	p	Term Value[a]
0	0	0.5	e	0.0000	1	0.5	f	11.4101
0	1	1.5	e	11.4495	2	1.5	f	34.2612
0	2	2.5	e	34.3269	3	2.5	f	68.5235
0	3	3.5	e	68.6153	4	3.5	f	114.1716
0	4	4.5	e	114.2893	5	4.5	f	171.1719
0	5	5.5	e	171.3154	6	5.5	f	239.4825

Notes. [a] Units cm^{-1}.

(This table is available in its entirety in a machine-readable form in the online journal. A portion is shown here for guidance regarding its form and content.)

Table 9
Line Positions in Wavenumber Units

	^{24}MgH		^{25}MgH		^{26}MgH	
N	Calc[a]	$O-C$[a]	Calc	$O-C$	Calc	$O-C$
			0–0 Band, P_1 Branch			
1	19261.7857	−0.0028	19261.7278	...	19261.6911	...
2	19252.9353	0.0072	19252.9276	...	19252.9145	...
3	19243.8589	0.0061	19243.8694	...	19243.8771	...
4	19235.1092	0.0059	19235.1365	...	19235.1620	...
5	19226.9093	0.0047	19226.9519	...	19226.9927	...

Notes. [a] Results for ^{24}MgH taken from Shayesteh & Bernath (2011).

(This table is available in its entirety in a machine-readable form in the online journal. A portion is shown here for guidance regarding its form and content.)

Table 10
Line Positions in Wavelength Units

	^{24}MgH		^{25}MgH		N	Calc[b]
	$O-C$[a,b]	Calc[a]	$O-C$[a]	Calc[a]	$O-C$	
			0–0 Band, P_1 Branch			
1	5190.1813	0.0008	5190.1969	...	5190.2067	...
2	5192.5672	−0.0019	5192.5692	...	5192.5728	...
3	5195.0163	−0.0016	5195.0134	...	5195.0114	...
4	5197.3794	−0.0016	5197.3720	...	5197.3652	...
5	5199.5960	−0.0013	5199.5845	...	5199.5735	...

Notes.
[a] In air.
[b] Results for ^{24}MgH taken from Shayesteh & Bernath (2011).

(This table is available in its entirety in a machine-readable form in the online journal. A portion is shown here for guidance regarding its form and content.)

a rich spectrum in cool stars, with many atomic features (including the very strong Mg I b lines) and C_2 $d^3\Pi_g$–$a^3\Pi_u$ Swan system lines in addition MgH. These contaminating atomic and C_2 features severely blend or completely mask otherwise promising MgH lines, and previous stellar Mg isotopic studies have generally concentrated on a few features. For our synthetic spectrum tests, we assembled a linelist consisting of MgH lines from this study, C_2 from Brooke et al. (2013), and atomic lines from the Kurucz (2011) database.[7] We neglected lines of the C_2 isotopic form $^{12}C^{13}C$, since the parent $^{12}C_2$ lines are always weak in the Sun and stars considered here.

We applied this linelist to the solar spectrum, computing a synthetic spectrum using the current version of the LTE line analysis code MOOG (Sneden 1973) and adopting the Holweger & Mueller (1974) model solar atmosphere. In this procedure we adopted the solar-system Mg isotopic fractions given above. The resulting synthetic spectrum was compared to an electronic copy of the NSO Solar Flux Atlas (Wallace et al. 2011),[8] and the transition probabilities and wavelengths of atomic lines were altered until a satisfactory match between synthesis and observation was achieved. We assume that the transition strengths of the individual MgH lines are isotopologue independent.

We then produced synthetic spectra for HD 25329 and Arcturus with the iterated linelist and model atmospheres interpolated[9] from the ATLAS grid (e.g., Kurucz 2005). The synthetic spectra were Gaussian-smoothed to match the observed spectra. For the HD 25329 observational data we used a high resolution, high S/N spectrum observed by David K. Lai using Hamspec at Lick Observatory on 2011 August 18. The resolution is ∼80,000 and the S/N at 5150 Å is ∼220. For Arcturus we used the NOAO Arcturus Spectral Atlas (Hinkle et al. 2000).[10] Observations for the Arcturus atlas utilized the Kitt Peak coudé feed. The section of spectrum used was observed at a resolution of ∼140,000 with S/N > 500.

In Figure 3 we show observed and computed spectra for HD 25329. Panel (a) in the figure shows three MgH lines: 5134.3 Å 0–0 $Q_2$23, 5134.7 Å 0–0 $Q_1$23 blended with $R_2$11, and 5135.2 Å 0–0 $R_1$11. Panel (b) shows two MgH lines: 5139.8 Å 0–0 $R_2$10 and 5140.3 Å 0–0 $R_1$10. The latter transition is blended with much weaker 1–1 $R_2$4. These lines have been used in many previous analyses of this star. Inspection of this figure suggests that isotopic percentages ^{24}Mg:^{25}Mg:^{26}Mg ≃ 80:10:10 with probable uncertainties of ∼±2 in the minor isotope percentages are reasonable matches to the observed spectrum. This result is

[7] Available at http://kurucz.harvard.edu.
[8] Available digitally at http://diglib.nso.edu/ftp.html.
[9] Model interpolation software was kindly provided by Andy McWilliam and Inese Ivans.
[10] Available at ftp://ftp.noao.edu/catalogs/arcturusatlas/.

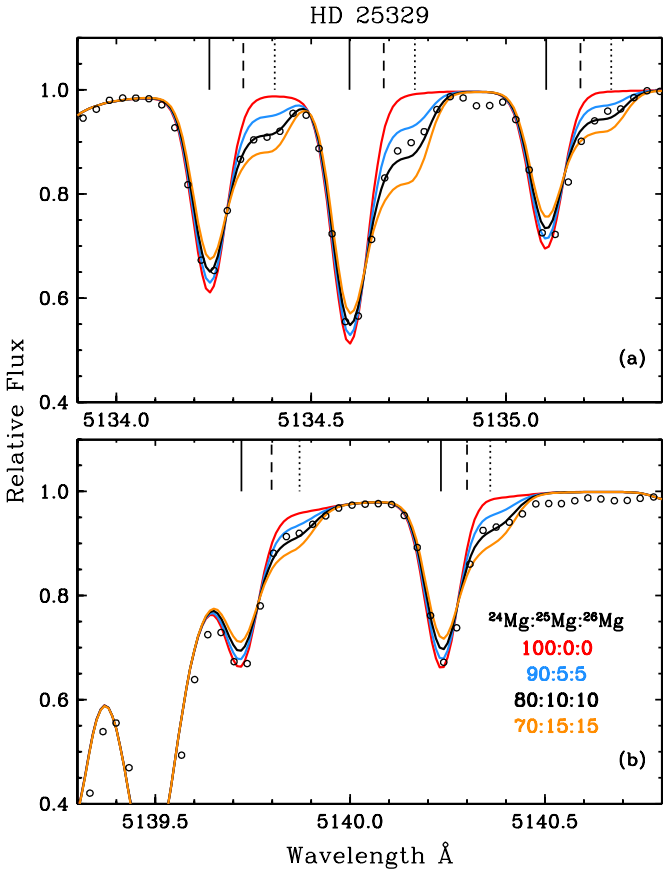

Figure 3. Comparison of observed and synthetic spectra for prominent MgH lines in the spectrum of the metal-poor main-sequence star HD 25329. Open circles represent the observations and solid colored lines represent the synthetic spectra. In panel (a) we show the triplet of MgH lines that has most often been employed to estimate Mg isotopic ratios, and in panel (b) we show two other nearby relatively MgH lines. The isotopic mixes are stated in panel (b).

(A color version of this figure is available in the online journal.)

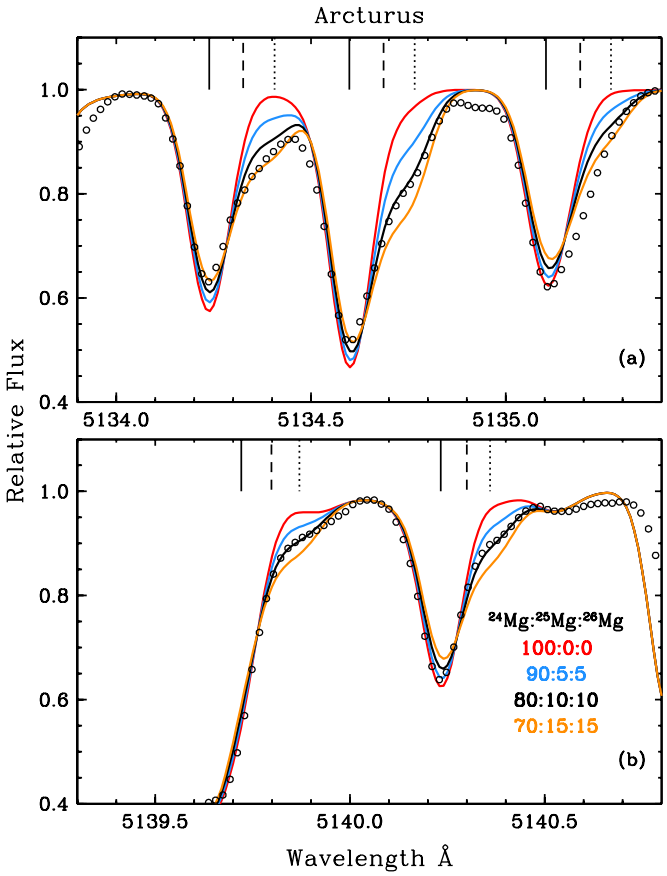

Figure 4. Comparison of observed and synthetic spectra for prominent MgH lines in the spectrum of the mildly metal-poor giant Arcturus. The symbols and lines are as in Figure 3.

(A color version of this figure is available in the online journal.)

in good agreement with the more detailed assessment of Yong et al. (2003): 84:8:8. (see also Gay & Lambert 2000). Figure 4 shows the same MgH lines in Arcturus. Although the MgH lines are of comparable depth to those of HD 25329, contaminating features are stronger. The obvious blend near 5135.2 Å renders that MgH triplet useless for an isotopic percentage assessment, and the continuum is difficult to place for the 5140.3 Å triplet. Nevertheless, for Arcturus we estimate ^{24}Mg:^{25}Mg:^{26}Mg $\simeq$ 80:10:10 from the 5134.7 and 5140.3 Å features. This is in good agreement with result from McWilliam & Lambert (1988): 82:9:9. It is clear that application of our new MgH linelist to two well-studied stars produces comparable isotopic percentages as those derived in previous analyses.

This project would not have been possible without the effort led by Dr. James W. Brault to build the McMath-Pierce FTS and subsequently to obtain hollow cathode spectra of many astrophysically important molecules. We thank Phil Weck for helpful discussions about laboratory MgH studies. L.W. thanks the NOAO emeritus program for the continued support of his research. The work at the University of York has been supported by funding from Leverhulme Trust of UK. P.B. thanks the NASA laboratory astrophysics program for partial support. The National Science Foundation grant AST-1211585 to C.S. provided partial support for, as well as motivation for, the research reported here. The National Optical Astronomy Observatory is operated by the Association of Universities for Research in Astronomy (AURA), under cooperative agreement with the National Science Foundation.

REFERENCES

Almy, G. M., & Crawford, F. H. 1929, PhRv, 34, 1517
Amiot, C., Maillard, J.-P., & Chauville, J. 1981, JMoSp, 87, 196
Asensio Ramos, A., & Trujillo Bueno, J. 2005, ApJL, 635, L109
Balfour, W. J. 1970, ApJ, 162, 1031
Balfour, W. J. 1980, JMoSp, 79, 507
Bergemann, M., & Gehren, T. 2008, A&A, 492, 823
Bergemann, M., Hansen, C. J., Bautista, M., & Ruchti, G. 2012, A&A, 546, A90
Bernath, P. F., Black, J. H., & Brault, J. W. 1985, ApJ, 298, 375
Boesgaard, A. M. 1968, ApJ, 154, 185
Bonnell, J. T., & Bell, R. A. 1993, MNRAS, 264, 334
Brooke, J. S. A., Bernath, P. F., Schmidt, T. W., & Bacskay, G. B. 2013, JQSRT, 124, 11
Brown, J. M., Colbourn, E. A., Watson, J. K. G., & Wayne, F. D. 1979, JMoSp, 74, 294
Bucchino, M. P., & Ziurys, L. M. 2013, JPCA, in press
Catanzaro, E. J., Murphy, T. J., Garner, E. L., & Shields, W. R. 1966, JRNBS, 70A, 453
Cottrell, P. L. 1978, ApJ, 223, 544
Douay, M., Rogers, S. A., & Bernath, P. F. 1988, MolPh, 64, 425
Edlén, B. 1953, JOSA, 43, 339
Gay, P. L., & Lambert, D. L. 2000, ApJ, 533, 260
GharibNezhad, E., Shayesteh, A., & Bernath, P. F. 2013, MNRAS, in press
Harmer, D. L., & Pagel, B. E. J. 1973, MNRAS, 165, 91
Hinkle, K., Wallace, L., Valenti, J., & Harmer, D. 2000, Visible and Near Infrared Atlas of the Arcturus Spectrum, 3727–9300 Å (San Francisco, CA: ASP)

Holweger, H., & Mueller, E. A. 1974, SoPh, 39, 19
Kurucz, R. L. 2005, MSAIS, 8, 14
Kurucz, R. L. 2011, CaJPh, 89, 417
McWilliam, A., & Lambert, D. L. 1988, MNRAS, 230, 573
Meléndez, J., & Cohen, J. G. 2007, ApJL, 659, L25
Mohan Rao, D., & Rangarajan, K. E. 1999, ApJL, 524, L139
Pavlenko, Ya. V., Harris, G. J., Tennyson, J., et al. 2008, MNRAS, 386, 1338
Reid, I. N., Kirkpatrick, J. D., Gizis, J. E., et al. 2000, AJ, 119, 369
Sansonetti, C. J. 2007, J. Res. Natl. Inst. Stand. Technol., 112, 297
Shayesteh, A., Appadoo, D. R. T., Gordon, I., Le Roy, R. J., & Bernath, P. F. 2004, JChPh, 120, 10002
Shayesteh, A., & Bernath, P. F. 2011, JChPh, 135, 094308
Shayesteh, A., Henderson, R. D. E., Le Roy, R. J., & Bernath, P. F. 2007, J. Chem. Phys. A, 111, 12495
Sneden, C. 1973, ApJ, 184, 839
Sneden, C. 1974, ApJ, 189, 493
Tomkin, J., & Lambert, D. L. 1980, ApJ, 235, 925
Wallace, L., Hinkle, K. H., Li, G., & Bernath, P. F. 1999, ApJ, 524, 454
Wallace, L., Hinkle, K. H., Livingston, W. C., & Davis, S. P. 2011, ApJS, 195, 6
Wallace, L., & Livingston, W. 2005, An Atlas of Sunspot Umbral Spectra in the Visible from 15000 to 25000 cm^{-1} (3920 to 6664 Å) (revised ed.; Tucson, AZ: NSO)
Weck, P. F., Schweitzer, A., Stancil, P. C., Hauschildt, P. H., & Kirby, K. 2003a, ApJ, 582, 1059
Weck, P. F., Schweitzer, A., Stancil, P. C., Hauschildt, P. H., & Kirby, K. 2003b, ApJ, 584, 459
Whaling, W., Anderson, W. H. C., Carle, M. T., Brault, J. W., & Zarem, H. A. 2002, J. Res. Natl. Inst. Stand. Technol., 109, 149
Wöhl, H. 1969, A&A, 3, 378
Wyller, A. A. 1961, ApJ, 134, 805
Yong, D., Aoki, W., & Lambert, D. L. 2006, ApJ, 638, 1018
Yong, D., Lambert, D. L., & Ivans, I. I. 2003, ApJ, 599, 1357
Ziurys, L. M., Barclay, W. L., Jr., & Anderson, M. A. 1993, ApJL, 402, L21